Scalable and highly selective graphene-based ion-exchange membranes with tunable permselectivity – Supporting Information

Anna Aixalà-Perelló[1,2], *Alessandro Pedico*[1], *Marco Laurenti*[1,2], *Enrica Fontananova*[3], *Sergio Bocchini*[2], *Ivan Vito Ferrari*[2], *Andrea Lamberti*[1,2*]

[1]Politecnico di Torino, Dipartimento di Scienza Applicata e Tecnologia (DISAT), Corso Duca Degli Abruzzi, 24, 10129 Torino, Italy

[2]Istituto Italiano di Tecnologia, Center for Sustainable Future Technologies, Via Livorno 60, 10144 Torino, Italy

[3]Institute on Membrane Technology of the National Research Council (ITM-CNR), Via P. Bucci, cubo 17/C, at University of Calabria, 87036 Rende (CS), Italy

*E-mail: andrea.lamberti@polito.it

SUPLEMENTARY RESULTS

XPS

The surface chemistry of GO membranes was investigated by X-Ray Photoelectron Spectroscopy (XPS).

For all the analyzed membranes, Supplementary Figure 1 shows the corresponding wide-energy XPS spectra while Supplementary Table 1 reports the relative atomic percentage for the detected elements.

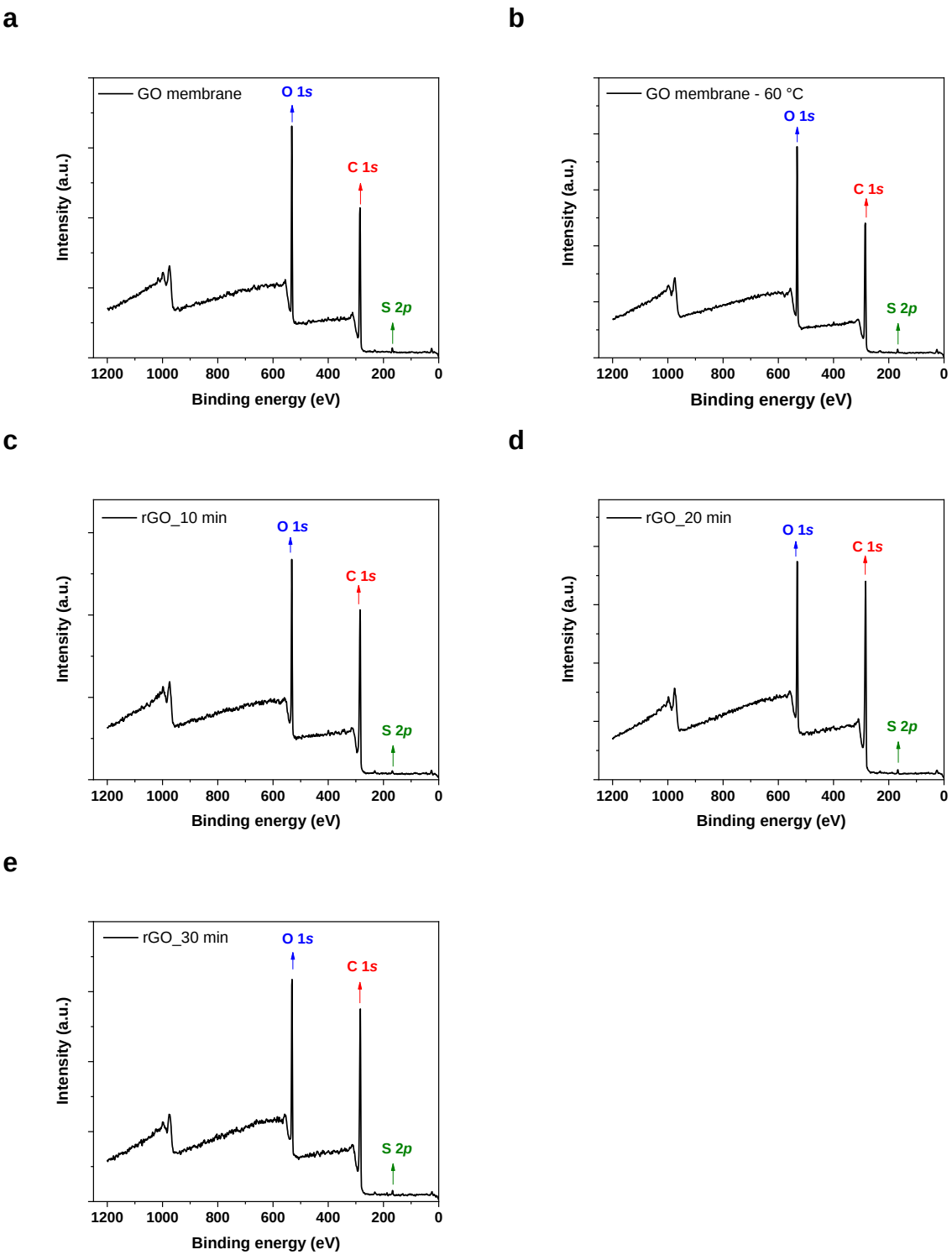

Supplementary Figure 1. Wide-energy XPS spectra of GO membranes: a as-prepared; **b** after thermal treatment at 60°C; **after UV light irradiation for: c** 10 min, **d** 20 min, and **e** 30 min.

Supplementary Table 1. Quantitative analysis of the GO membranes' chemical composition obtained from wide-energy XPS scan analysis.

Sample	C, At%	O, At%	S, At%
GO	68.07 ± 0.34	31.35 ± 0.34	0.57 ± 0.10
GO@60°C	68.11 ± 0.30	31.37 ± 0.30	0.52 ± 0.07
rGO UV 10min	71.80 ± 0.41	27.76 ± 0.41	0.44 ± 0.09
rGO UV 20 min	74.52 ± 0.32	24.91 ± 0.32	0.56 ± 0.08
rGO UV 30 min	74.07 ± 0.41	25.42 ± 0.40	0.51 ± 0.09

a **b**

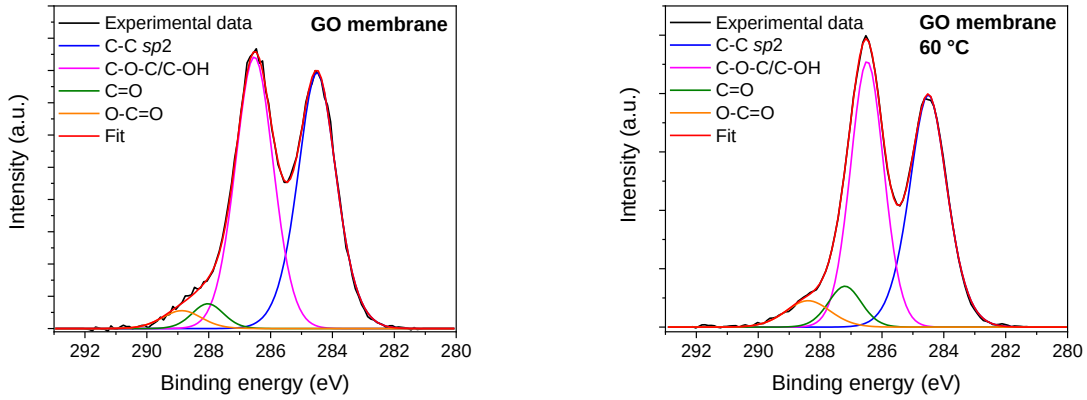

Supplementary Figure 2. High-resolution C1s XPS spectra of GO membranes: a as-prepared; **b** after thermal treatment for 60°C.

The HR C1*s* XPS spectra of the as-prepared GO membrane and the one dried at 60 °C are reported in Supplementary Figure 2. No relevant differences between the two samples can be found. Therefore, the mild-temperature treatment does not induce any change in the chemistry of the starting membrane nor induce any GO reduction.

Supplementary Table 2. Semi-quantitative results obtained from the deconvolution of HR C1*s* peak for GO membranes.

	%Area				
Sample	C-C sp_2	C-O-C/C-OH	C=O	O-C=O	satellite
GO	45.04	46.14	5.66	3.16	-
rGO-UV10	58.58	29.61	5.43	4.81	1.57
RGO-UV20	59.60	28.50	4.95	5.46	1.49
RGO-UV30	58.44	29.21	5.62	5.31	1.42
GO@60°C	44.10	43.47	6.63	5.80	-

Contact angle

Surface energy of membranes was evaluated by contact angle. Supplementary Figure 3 shows an example of the images used to make the measurement with water and diiodomethane.

Supplementary Figure 3. Contact angle of GO membrane measurement with: a water, **b** CH_2I_2.

EIS

EIS measurements were pursued in a frequency range from 10^5 Hz to 0.1 Hz (Supplementary Figure 5a). The spectra showed from Supplementary Figures 5-11 focus just on the region in which the curve intercepts the real axis of the impedance (Z').

a **b**

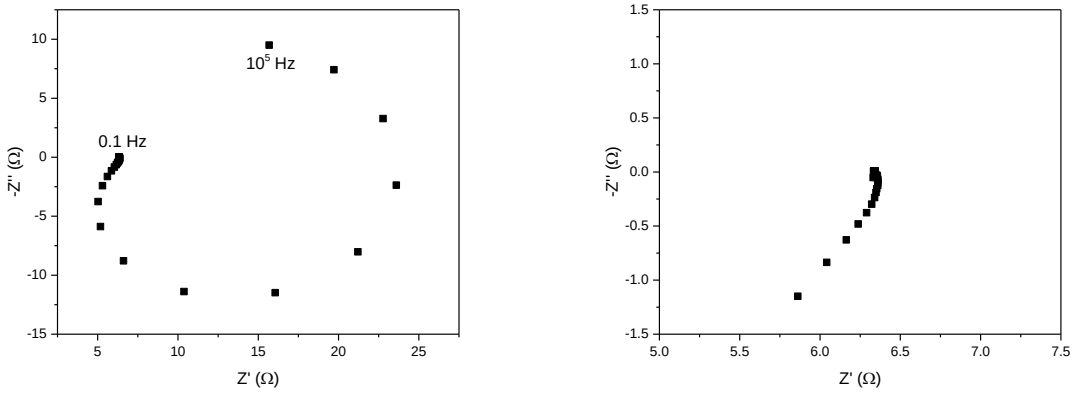

Supplementary Figure 4. Nyquist plot of a blank measurement. a all the spectra from 10^5 Hz to 0.1 Hz **b** particular of the spectra in the region of the intercept with the real axys.

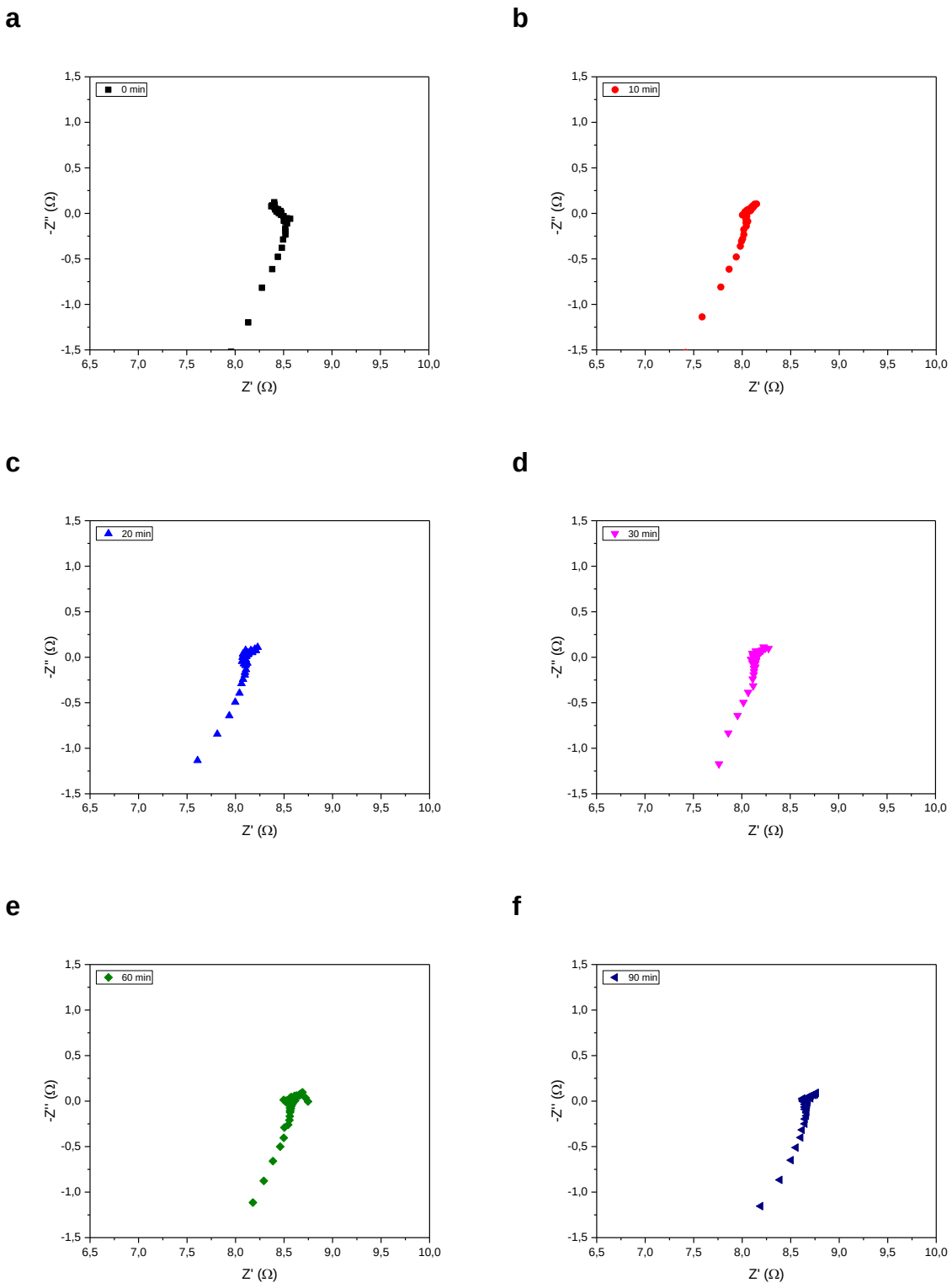

Supplementary Figure 5. Nyquist plot of GO-20 at different times. a 0 min **b** 10 min **c** 20 min **d** 30 min **e** 60 min **f** 90 min.

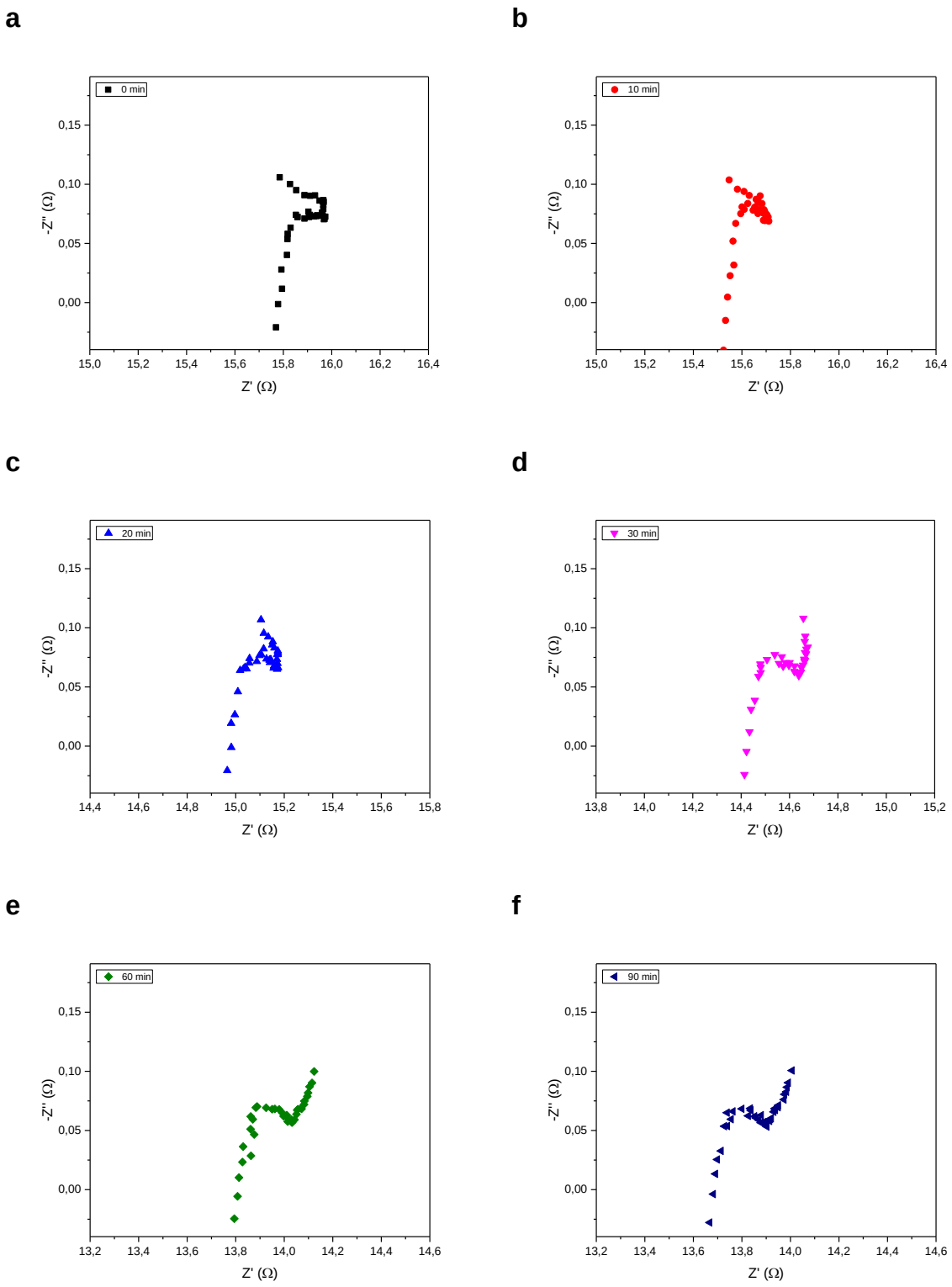

Supplementary Figure 6. Nyquist plot of GO-40 at different times. a 0 min **b** 10 min **c** 20 min **d** 30 min **e** 60 min **f** 90 min.

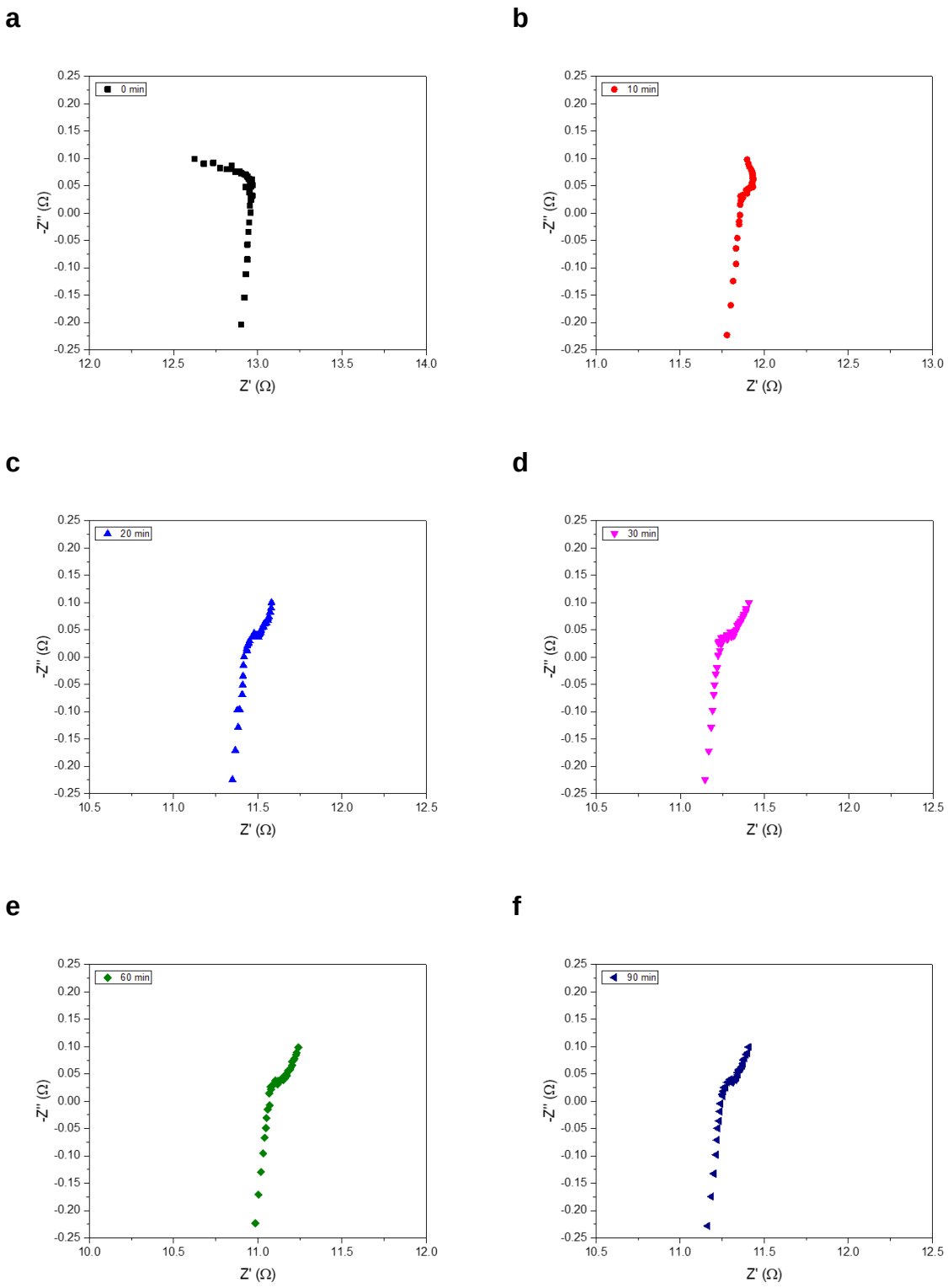

Supplementary Figure 7. Nyquist plot of rGO-UV20 at different times. a 0 min **b** 10 min **c** 20 min **d** 30 min **e** 60 min **f** 90 min.

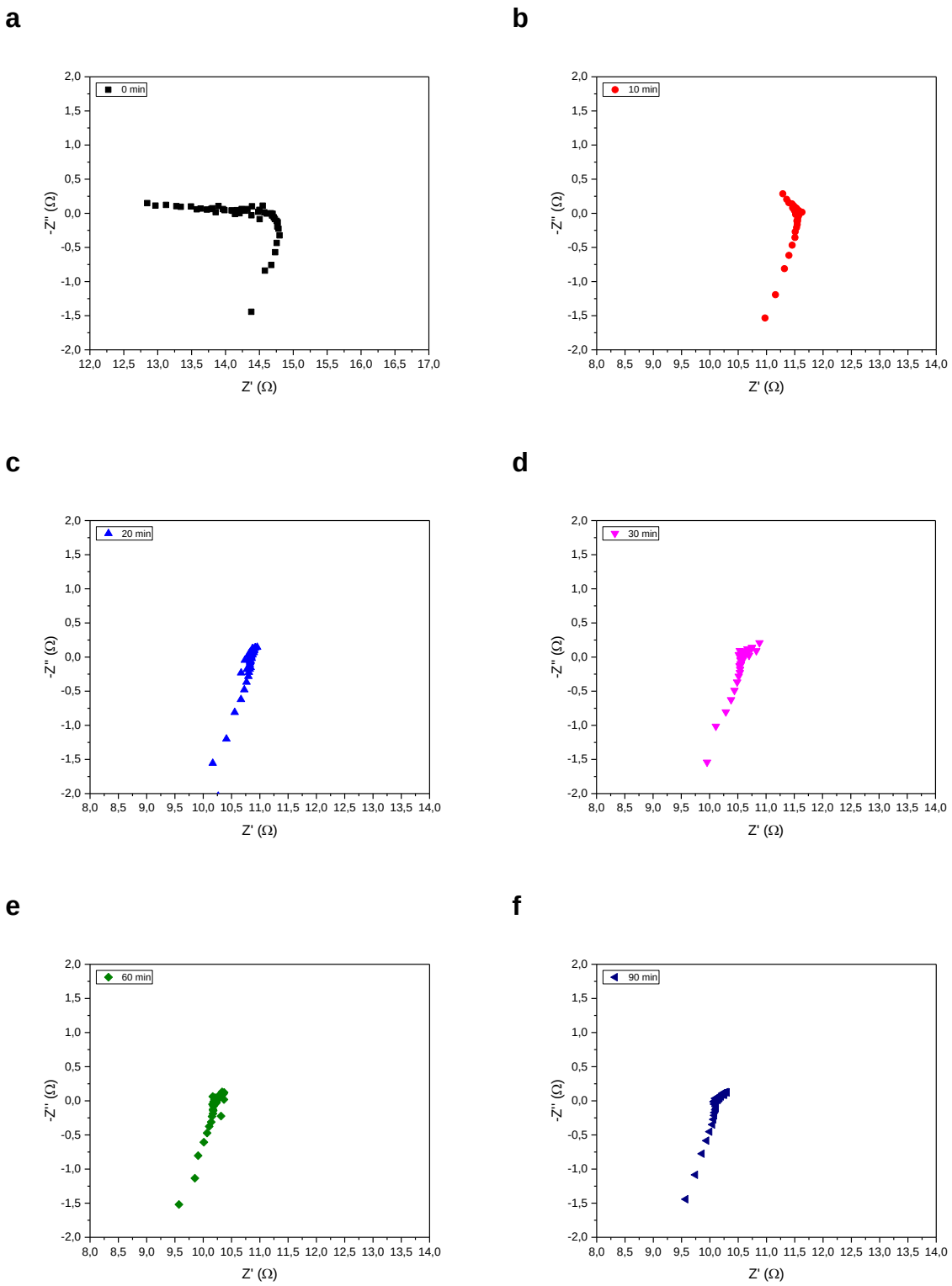

Supplementary Figure 8. Nyquist plot of GOPVA-20 at different times. a 0 min **b** 10 min **c** 20 min **d** 30 min **e** 60 min **f** 90 min.

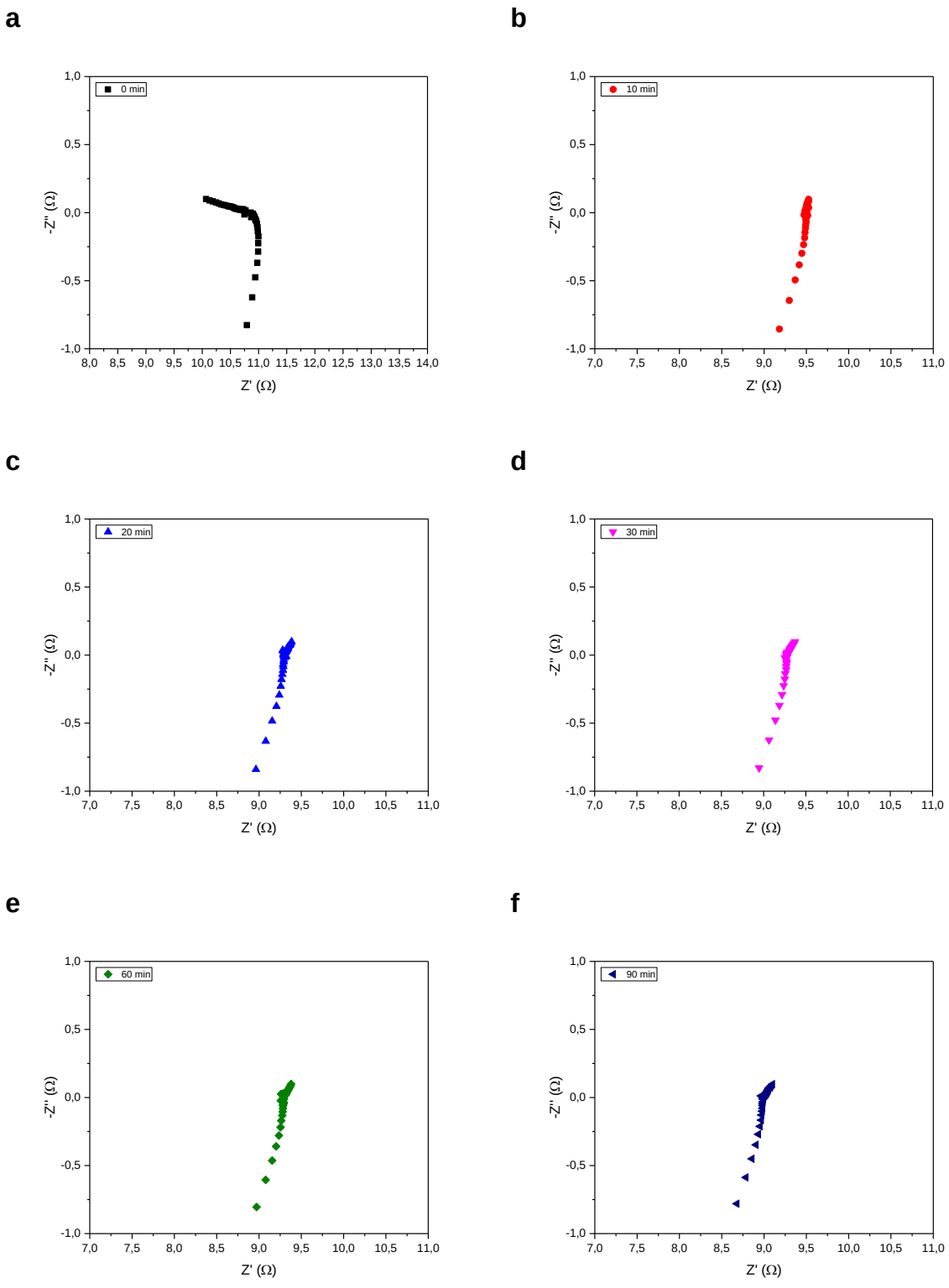

Supplementary Figure 9. Nyquist plot of GOPVP-20 at different times. **a** 0 min **b** 10 min **c** 20 min **d** 30 min **e** 60 min **f** 90 min.

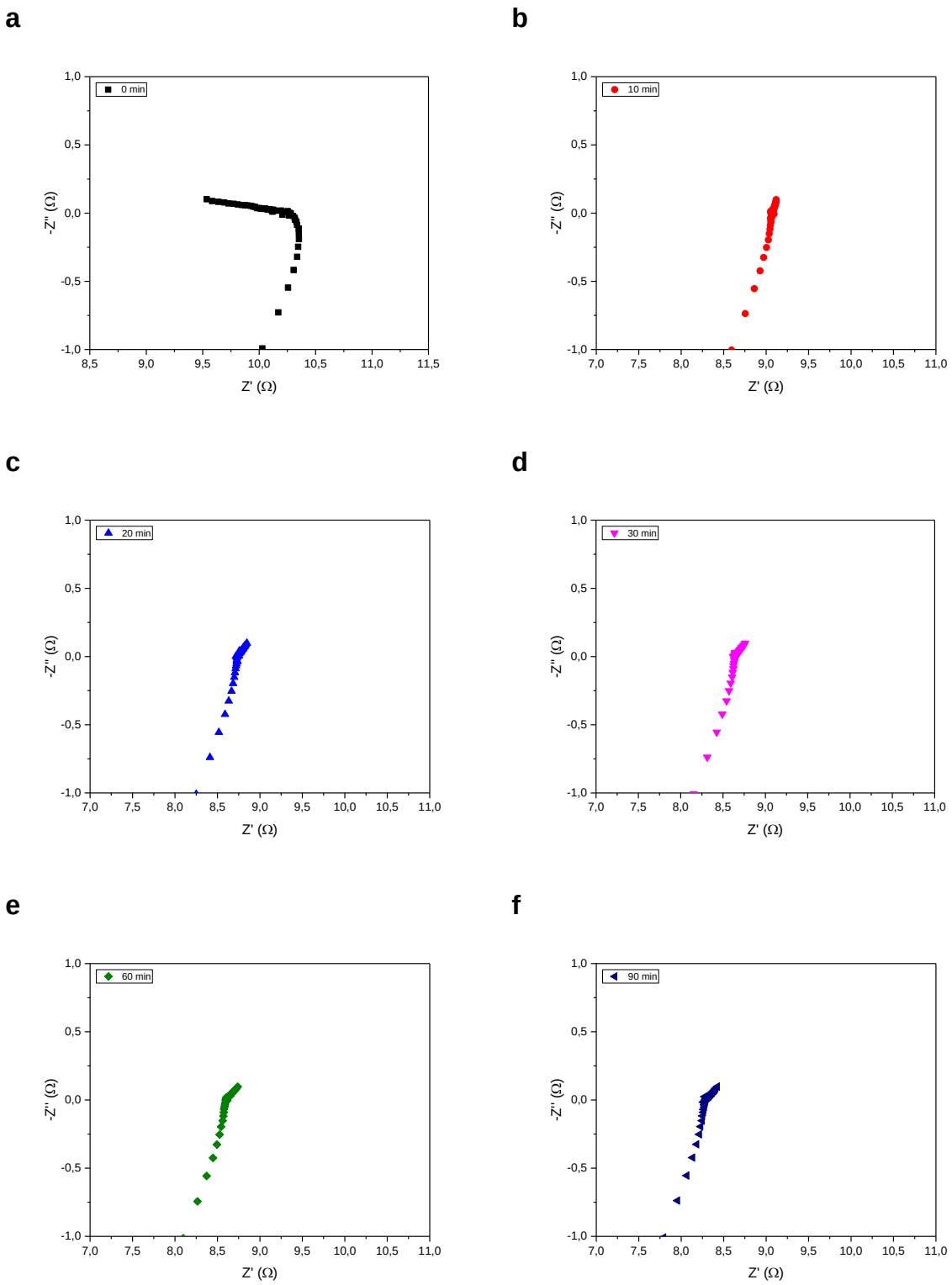

Supplementary Figure 10. Nyquist plot of GOSPEEK10-20 at different times. a 0 min **b** 10 min **c** 20 min **d** 30 min **e** 60 min **f** 90 min.

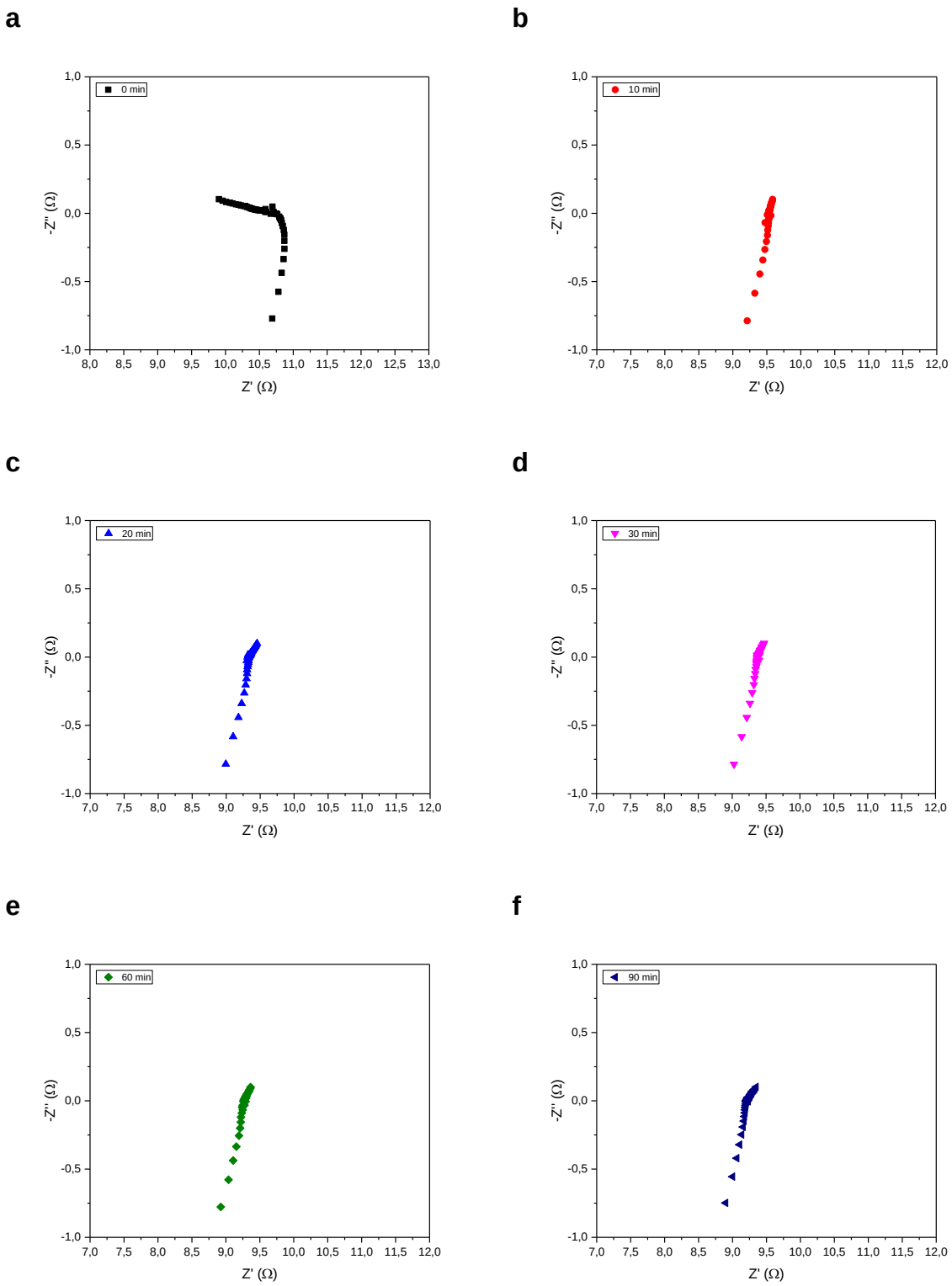

Supplementary Figure 11. Nyquist plot of GOSPEEK20-20 at different times. a 0 min **b** 10 min **c** 20 min **d** 30 min **e** 60 min **f** 90 min.

Transference number

Ion selectivity of membranes can also be calculated in terms of transference number (t_+), another parameter often used to evaluate IEM's performance[1–3].

$$2t_+ - 1 = \frac{E_{mem}}{\frac{RT}{zF}\ln\left(\frac{\gamma_c c_c}{\gamma_d c_d}\right)} \quad \textbf{(1)}$$

Where *R, T, z, F, γ* and *c* stand for the gas constant, the temperature, the Faraday constant, the activity coefficient of ions and the concentration. Instead, *c* and *d* represent the concentrated and diluted electrolytes.

Permselectivity

Theoretical potential needed to calculate permselectivity of membranes is calculated as follows [4]:

$$E_{the} = -\frac{RT}{z_g F} ln \frac{\gamma_c c_c}{\gamma_d c_d} \quad \textbf{(2)}$$

Where *T* is the absolute temperature, *R* is the universal gas constant, *F* is the Faraday constant, z_g is the valence of the counter-ion, *c* is the concentration, *γ* is the activity coefficient of solutions and superscripts *c* and *d* correspond to concentrated and diluted solutions.

Liquid junction potential encountered in the reference electrodes was calculated by Henderson equation [5]. Ionic mobilities at infinite dilution were used.

$$E_j = \frac{\sum_i \frac{|z_i|u_i}{z_i}[c_i(2) - c_i(1)]}{\sum_i |z_i|u_i[c_i(2) - c_i(1)]} \frac{RT}{F} ln \frac{\sum_i |z_i|u_i c_i(1)}{\sum_i |z_i|u_i c_i(2)} \quad \textbf{(3)}$$

Supplementary Table 3 shows theoretical potential values obtained with different electrolyte solutions and gradients. Supplementary Table 4 presents the Liquid Junction Potential calculation for all electrolytes.

Supplementary Table 3. Calculated theoretical potential from Nernst equation.

Salt	Concentrations	γ_{conc}	$\gamma_{diluted}$	E_{the}
LiCl[6]	0.5/0.1	0.739	0.789	-39.67
NaCl[7]	0.5/0.1	0.6797	0.7773	-37.90
KCl[8]	0.5/0.1	0.649	0.768	-37.02
KCl[8]	1/0.01	0.604	0.901	-108.04
KCl[8]	1/0.1	0.604	0.768	-52.99
KCl[8]	1/0.5	0.604	0.649	-15.96
$MgCl_2$[9]	0.5/0.1	0.4887	0.5202	-39.75
$CaCl_2$[9]	0.5/0.1	0.4472	0.5	-38.48

Supplementary Table 4. Calculated junction potential from Henderson equation.

Filling solution	Bulk solution	Bulk concentrations	$E_{j,conc}$ (mV)	$E_{j,dil}$ (mV)	ΔE_j (mV)
KCl (3M)	LiCl	0.5/0.1	-1.37	1.06	-2.43
KCl (3M)	NaCl	0.5/0.1	-0.59	1.27	-1.85
KCl (3M)	KCl	0.5/0.1	0.89	1.69	-0.80
KCl (3M)	KCl	1/0.01	0.54	2.83	-2.28
KCl (3M)	KCl	1/0.1	0.54	1.69	-1.14
KCl (3M)	KCl	1/0.5	0.54	0.89	-0.34
KCl (3M)	MgCl2	0.5/0.1	-4.11	-0.22	-3.89
KCl (3M)	CaCl2	0.5/0.1	-3.72	-0.11	-3.61

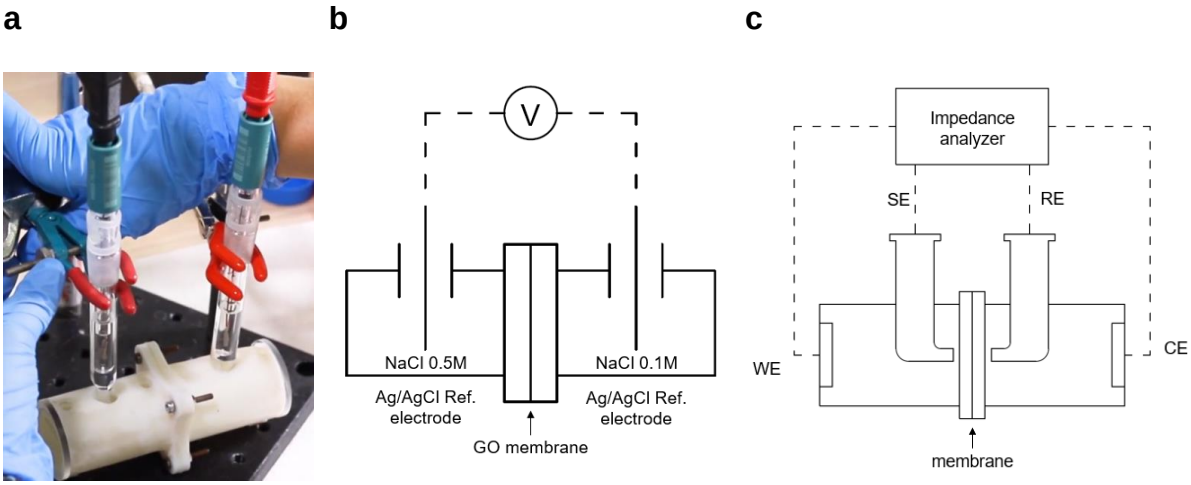

Supplementary Figure 12. Electrochemical set-ups used. a Picture of the experimental set-up used to measure the permselectivity **b** Scheme of the experimental set-up used to measure the permselectivity **c** Scheme of the experimental set-up used to measure the ionic resistance.

Permselectivity was measured using different salts as electrolytes to see the effect of size and charge (Supplementary Figure 13).

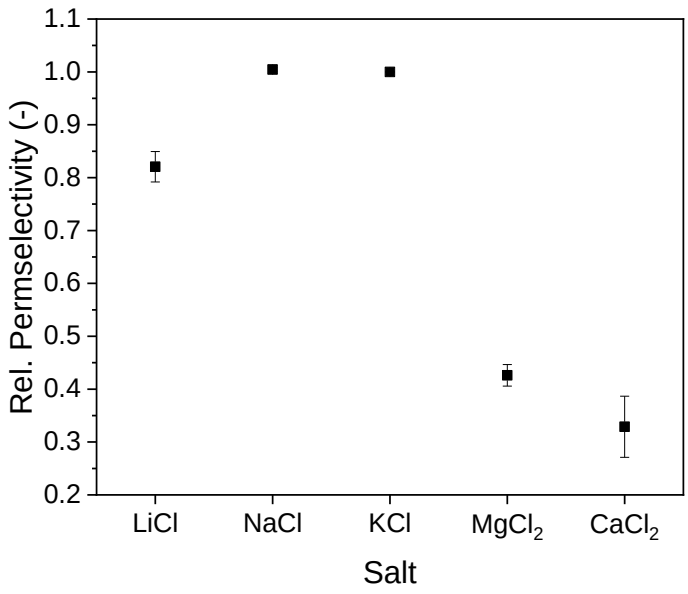

Supplementary Figure 13. Permselectivity of GOPVP-20 using different salts.

Stress-strain measurements

Stress-strain measurements were performed to GO-20 and GOPVP-20 membranes to compare their mechanical performance. Young's modulus, strain at break and stress at break were evaluated showing an increase of performances for all parameters when adding the binder.

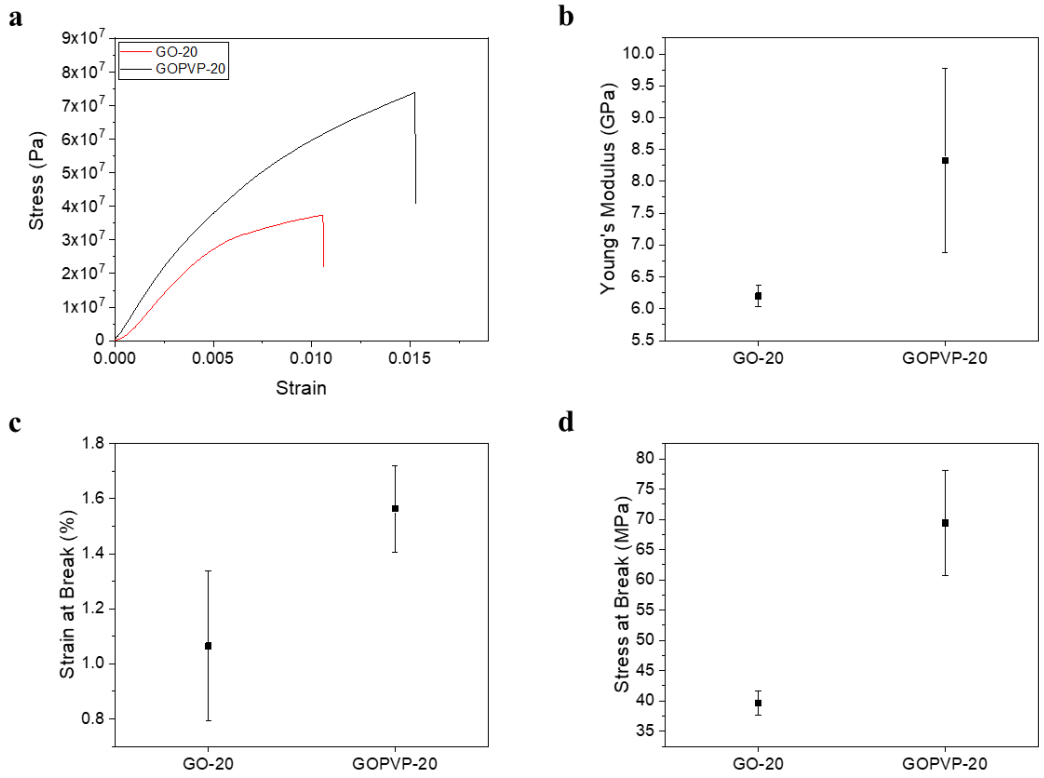

Supplementary Figure 14. Mechanical properties of go-20 and GOPVP-20 membranes. a Stress-strain measurement. **b** Young's modulus of membranes. c Strain at break of membranes. **d** Stress at break of membranes.

SUPPLEMENTARY REFERENCES

1. Gao, J. *et al.* High-performance ionic diode membrane for salinity gradient power generation. *J Am Chem Soc* **136**, 12265–12272 (2014).
2. Ji, J. *et al.* Osmotic Power Generation with Positively and Negatively Charged 2D Nanofluidic Membrane Pairs. *Advanced Functional Materials* **27**, 1603623 (2017).
3. Lee, S. W., Kim, H. J. & Kim, D. K. Power generation from concentration gradient by reverse electrodialysis in dense silica membranes for microfluidic and nanofluidic systems. *Energies* **9**, (2016).
4. Kingsbury, R. S., Flotron, S., Zhu, S., Call, D. F. & Coronell, O. Junction Potentials Bias Measurements of Ion Exchange Membrane Permselectivity. *Environmental Science and Technology* **52**, 4929–4936 (2018).
5. Atkins, Peter; de Paula, J. *Elements of Physical Chemistry*. (Great Britain by Oxford University Press, 2009).
6. Taghikhani, V., Modarress, H. & Vera, J. H. Individual anionic activity coefficients in aqueous electrolyte solutions of LiCl and LiBr. *Fluid Phase Equilibria* **166**, 67–77 (1999).
7. Ghalami-Choobar, B. & Nosrati Fallahkar, T. Mean activity coefficients measurement of sodium chloride and thermodynamic modeling of sodium chloride and polysodium acrylate aqueous mixtures at T=(298.2 and 303.2)K. *Fluid Phase Equilibria* **378**, 51–59 (2014).
8. Hamer, W. J. & Yung chi, Y. Osmotic Coefficients and Mean Activity Coefficients of Uni univalent Electrolytes in Water at 25°C. *Journal of Physical and Chemical Reference Data* **1**, 1047 (1972).

9. Rodil, Eva; Vera, J. H. Individual activity coefficients of chloride ions in aqueous solutions of MgCl2 CaCl2 and BaCl2 at 298.2K.pdf. *Fluid Phase Equilibria* **187–188**, 15–27 (2001).